Open Archive Toulouse Archive Ouverte (OATAO)

OATAO is an open access repository that collects the work of Toulouse researchers and makes it freely available over the web where possible

This is an author's version published in: **http://oatao.univ-toulouse.fr/23288**

Official URL: https://doi.org/10.1007/s10973-018-7292-x

Thermal, mechanical and dielectric behaviour of poly(aryl ether ketone) with low melting temperature

Jérémie Audoit[1] · Lisa Rivière[1] · Jany Dandurand[1] · Antoine Lonjon[1] · Eric Dantras[1] · Colette Lacabanne[1]

Abstract
New poly(aryl ether ketone)s (PAEKs) with a low melting temperature (relative to PEEK) are of interest in order to simplify the manufacturing of high-performance polymers or composites. In this study, we propose to investigate the physical properties of a new PAEK from Victrex, namely PAEK LM. Combinations of thermal analyses were used as follows: standard and modulated temperature differential scanning calorimetry, dynamic mechanical analysis, dynamic dielectric analysis and guarded hot plate technique. We found that the global mechanical, dielectric and thermal properties are very similar to the PEEK reference. The glass transition temperature was observed in the same range than PEEK ($\sim$ 150 °C) while the melting temperature T_m was measured at 307 °C for PAEK LM which is about 35 °C below the melting temperature of PEEK. The degree of crystallinity of PAEK LM was found to be 27% while for PEEK it is 38%, depending on the processing conditions. This work explored crystalline structure–property relationships to explain the behaviour of PAEK LM.

Keywords Poly(aryl ether ketone) · DSC · Dynamic mechanical analysis · Dynamic dielectric spectroscopy · Thermal conductivity

Introduction

Poly(aryl ether ketones) (PAEKs) are high-performance thermoplastic semi-crystalline polymers. Poly(ether ether ketone) (PEEK) and poly(ether ketone ketone) (PEKK) excited interests in various sectors because of their good mechanical properties and their solvent resistance. Their high-mechanical properties made them suitable as structural material for medical applications [1, 2], polymer blends for gas separation membranes [3], nanocomposites [4–7] and polymer matrices for high-performance composites [8–11]. The thermal stability of PAEKs was widely investigated [12, 13]. Physical properties of PEEK and PEKK were analysed by solid state NMR [14], XRD [15], DSC [16–19], mechanical relaxation [20–22] and dielectric analysis [23–25].

✉ Eric Dantras
eric.dantras@univ-tlse3.fr

1 CIRIMAT, Université de Toulouse, CNRS, Physique des Polymères, 118 route de Narbonne, 31062 Toulouse Cedex 09, France

High-temperature processing is required for PAEK polymer/composites [23]. Decreasing melting temperature of thermostable polymers has a potential interest to facilitate PAEK polymer processing in order to reduce manufacturing costs. The lowering of melting temperature has been already successfully achieved for PEKK by the introduction of precursor with different configurations during the Friedel–Crafts polymerization [26]. A fixed ratio of terephthalic (*T*) over isophthalic (*I*) moieties (*T/I*) enables the melting temperature of the resulting polymer to be tuned with a limited influence on the glass temperature or mechanical properties [21]. Gardner [27] reported a range of melting temperatures between 300 and 400 °C as a function of the *T/I* ratio. During polymerization, the modification of configurations by the substitution of *T* entities by *I* entities induced conformational defects resulting in local disorder. These conformational defects lead to a decrease in melting temperature and degree of crystallinity [21, 28].

Tuning the melting temperature by chemical modifications of the repeating unit generally increases the solubility of the modified-PEEK in organic solvents depending on the

substituted moieties. Recently, Victrex (UK) developed a new PEEK-like polymer: VICTREX AE™ 250. It is supposed to have similar physical properties to PEEK with a lower melting temperature. To our knowledge, no configurational variations have been reported for PEEK. In this work, we propose to compare physical structure, thermal mechanical and dielectric behaviours of AE™ 250 and PEEK and to highlight similarities and differences.

Materials and methods

Materials

PEEK (150 µF) and VICTREX AE™ 250 grades (labelled PAEK LM) were supplied by Victrex as ultra-fine powders. Polymer samples were processed directly from powder for 15 min at 360 and 400 °C for PAEK LM and PEEK, respectively. Three thermal histories were explored. "Quenched" samples were obtained by fast cooling from the melt into a cold water bath; "slowly cooled" films were obtained by slow air-cooling from the melt; and "annealed" samples were obtained by annealing for 2 h "slowly cooled" samples at various temperatures from 180 to 250 °C.

Methods

Standard differential scanning calorimetry

Differential scanning calorimetry was performed using DSC7 from PerkinElmer. Samples are thin discs of 6 mm in diameter, with a mass ranging between 5 and 15 mg. Three cycles are performed on each sample from 50 to 360 °C at a rate of 10 °C min^{-1}. The first-order transitions were measured at the peak maximum. Crystallinity ratio χ was determined from melting enthalpy ΔH_m according to Eq. (1).

$$\chi(\%) = \frac{\Delta H_m - \Delta H_{cc}}{\Delta H_\infty} \tag{1}$$

ΔH_{cc} is the cold crystallization enthalpy. It was used for quenched samples only.

ΔH_∞ is the theoretical melting enthalpy of the 100% crystalline polymer [16]. The PEEK value $\Delta H_{\infty PEEK} = 130$ J g^{-1} was utilized.

Modulated temperature differential scanning calorimetry

Modulated temperature differential scanning calorimetry (MT-DSC) allowed us to determine the specific heat capacity in quasi-isothermal conditions. It relies on the superimposition of a modulated temperature programme to isotherms and the analysis of the sample modulated heat flow response. Separation of the in-phase and out-of-phase responses from total heat flow leads to specific heat capacity determination. Specific heat capacity c_p is proportional to the modulated in-phase heat flow amplitude A_{HF} and the modulated temperature amplitude A_T far from any thermal event, according to the following equation [29]:

$$c_p = K \frac{A_{HF}}{A_T} \tag{2}$$

K is the calibration constant determined by a run with standard sapphire. It accounts for thermal responses of the reference, pans and furnace. PEEK- and PAEK LM-specific heat capacities were determined with the MT-DSC 2920 from TA Instruments at 19, 34 and 48 °C. Samples were discs of slowly cooled polymers with a diameter of 6 mm, a thickness less than 500 µm and a mass ranging from 11.7 to 20.6 mg, encapsulated in aluminium pans. An empty aluminium pan has been used as reference. Measurements were performed with a temperature amplitude of 1 °C and modulation period of 100 s to ensure uniform heat flow across the sample [30]. Calibration runs with sapphire were performed before each measurement.

Guarded hot plate method

In the guarded hot plate method, a cylindrical sample is stacked between two plates imposing a temperature gradient ΔT across it. Resulting heat flow ϕ is measured with a calorimeter placed under the stack, and the thermal conductivity, λ, is determined according to the following equation based on Fourier's law:

$$\lambda = \frac{\phi}{\Delta T} \times \frac{e}{S} \tag{3}$$

e is the sample thickness and S its cross section. A guard annihilates heat losses through samples' lateral surface. The guarded hot plate apparatus DTC 300 from TA Instrument was used to measure PEEK and PAEK LM thermal conductivities at 25, 50, 80, 150, 200 and 250 °C. Samples were discs with 50 mm in diameter and a thickness varying from 2.4 to 2.7 mm. Thermal conductivity measurements were performed after annealing at 250 °C during 30 min to avoid bias due to crystallites reorganization during measurements above the glass transition temperature.

Dynamic mechanical analyses

Dynamic mechanical analyses were performed using an ARES G1 strain-controlled rheometer. Experiments were carried out in rectangular torsion mode, over the

temperature range from -135 to $250\,°C$ at constant angular frequency $\omega = 1$ rad s^{-1}, with a heating rate of $3\,°C$ min^{-1}. Parallelepiped samples (35 mm $\times$ 10 mm $\times$ $500\,\mu m$) are processed by a hot-press. The conservative $G'_\omega(T)$ and dissipative $G''_\omega(T)$ moduli were determined for a 0.1% constant strain.

Dynamic dielectric analyses

Dynamic dielectric analyses were performed using broadband dielectric spectroscopy. Polymer films were elaborated with 40 mm in diameter and a thickness between 60 and $100\,\mu m$. The complex permittivity $\varepsilon_T^*(\omega)$ is isothermally measured, with a Novocontrol Alpha-A impedance analyser on the 10^{-2}–10^6 Hz frequency range in the temperature range $-150/250\,°C$. Relaxation modes are fitted with the Havriliak–Negami equation [31]:

$$\varepsilon_T^*(\omega) = \varepsilon_\infty + \frac{\varepsilon_0 - \varepsilon_\infty}{\left(1 + (i\omega\tau_{HN})^{\alpha_{HN}}\right)^{\beta_{HN}}} \tag{4}$$

ε_0 and ε_∞ are, respectively, the permittivity at zero and infinite frequency. τ_{HN} is the relaxation time; α_{HN} and β_{HN} are the Havriliak–Negami parameters.

The relaxation time is plotted as a function of $1/T$, on an Arrhenius diagram. Sub-glass relaxations are fitted with the Arrhenius equation (Eq. 5).

$$\tau_{Arr}(T) = \tau_0 \cdot \exp\left(-\frac{E_a}{RT}\right) \tag{5}$$

where τ_0, E_a and R are the pre-exponential factor, the activation energy and the gas constant, respectively. Above the dielectric manifestation of the glass transition, relaxation times are fitted with the Vogel–Tammann–Fulcher equation (VTF) (Eq. 6).

$$\tau_{VTF}(T) = \tau_0 \exp\left(\frac{1}{\alpha_f(T - T_\infty)}\right) \tag{6}$$

where τ_0 is the pre-exponential factor, α_f is the free volume thermal expansion coefficient, T_∞ is the critical temperature.

Above the dielectric manifestation of the glass transition temperature, the Maxwell–Wagner–Sillars phenomenon is partially hidden by the conductivity—mainly ionic conductivity for PEEK polymer [24]. The Kramers–Kronig transform was used to calculate the dissipative part of the permittivity ε''_{KK} from the values of the real part of the permittivity ε'.

$$\varepsilon''_{KK}(\omega_0) = \frac{2}{\pi} \int_0^\infty \varepsilon'(\omega) \frac{\omega_0}{\omega^2 - \omega_0^2} d\omega \tag{7}$$

Results and discussion

Physical structure

Quenched PAEK

DSC analysis highlights the physical structure differences between PEEK and PAEK LM. Quenched samples show three thermal events: the glass transition at T_g, the exothermic cold crystallization at T_{cc} and the endothermic melting at T_m.

Main differences in cold crystallization and melting, between quenched PEEK or PAEK LM, are shown in Fig. 1. Parameters extracted from the analysis of the curves are reported in Table 1. The PAEK LM melting temperature is about $35\,°C$ lower than for PEEK; the cold crystallization is observed almost $15\,°C$ above the one of PEEKs. Contrarily, the glass transition temperature is the same for both polymers ($\sim 150\,°C$). The same behaviour (decrease of T_m for a stable T_g) was already reported for PEKK [27]. It is pertinent to report here that, when the T/I ratio of PEKK increases, the melting temperature also increases while the cold crystallization temperature decreases. Such data emphasized the key role of configurational order.

In the case of quenched samples, the crystallinity ratio was 6 and 10% for PAEK LM and PEEK, respectively (Table 1). PAEK LM crystallization kinetic is rapid (< 2 min), which is consistent with results reported for PEEK [17] or PEKK with T/I ratio of at least 70/30. Results showed that such rapid cooling rates ($100\,°C$ min^{-1}) are not sufficient to prevent crystallization. PAEK LM crystallization kinetic is faster than for PEEK. The literature shows that the PEKK crystallization is tunable when the cooling rates are between 10 and $60\,°C$ min^{-1} [21]. The crystallization kinetics of PAEK LM will be investigated in a future work.

The cold crystallization was observed at 169 and $182\,°C$ for PEEK and PAEK LM, respectively. A similar behaviour was described for PEKK: the cold crystallization temperature was reported to increase from 205 to $250\,°C$ when the T/I ratio decreases, i.e. upon the increase in configurational defects [21]. As for PEKK with low T/I ratio, a possible explanation for the increased crystallization temperature of PAEK LM is the decrease in polymer chain symmetry.

PAEK LM samples crystallized from the glass have a crystallinity ratio around 26%, close to the value obtained for melt-crystallized samples ($\chi = 27\%$), indicating the PAEK LM quickly crystallizes close to its maximum crystallinity ratio. The crystallinity ratio of cold-crystallized PEEK reached a higher value $\chi_{PEEK} = 38\%$. While
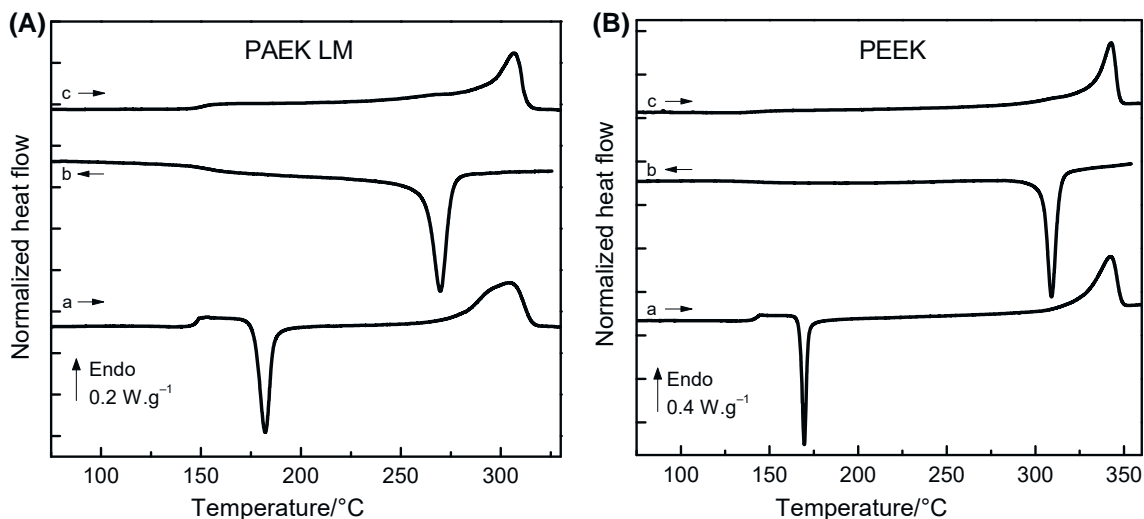
Fig. 1 DSC curves for **A** PAEK LM and **B** PEEK for heating and cooling rate of 10 °C min^{-1}. For each quenched polymer, (a) is the first heating curve, (b) is the cooling scan, and (c) is the second heating curve

Table 1 Transitions temperatures, crystallization enthalpies, crystallinity ratio and heat capacity jump of quenched PEEK and PAEK LM

	T_g/°C	T_{cc}/°C	ΔH_c/J g^{-1}	T_m/°C	χ/%	T_{cryst}/°C	ΔC_p/J g^{-1}
PEEK	142 ± 2	169 ± 1	− 30 ± 2	342 ± 2	10 ± 2	308 ± 2	0.30 ± 0.02
PAEK LM	147 ± 1	182 ± 1	− 25 ± 2	305 ± 1	6 ± 2	265 ± 1	0.29 ± 0.02

Standard deviations were determined from the variability over various samples

crystallized from the melt, the exotherm was monitored at 264 °C for PAEK LM and 308 °C for PEEK. The ratio T_m/T_c was found to be in the same range for both polymers.

Slowly cooled PAEK

DSC analyses of slowly cooled samples are reported in Fig. 2. Glass transition temperature of PAEK LM is measured at 151 and 148 °C for PEEK, slightly higher compared with their respective quenched samples. The T_g increase is attributed to the presence of the crystalline phase, which reduces the amorphous phase mobility. The PAEK LM glass transition temperature is in the same range of PAEK polymers: PEEK (Table 1), PEKK [18] and PEK [32]. The percentage of rigid amorphous fraction (RAF) was determined with Eq. (8) according to Ref. [33]. It was determined to be 22 ± 2 and 25 ± 2% for PEEK and PAEK LM, respectively. These values suggest that both polymers have a similar local order.

$$\text{RAF} = 1 - \chi_c - \text{MAF} = 1 - \chi_c - \frac{\Delta_{cp}}{\Delta_{cp_0}} \tag{8}$$

The melting temperature is measured at 307 °C for PAEK LM and at 342 °C for PEEK. The melting temperature of PAEK LM is 40 °C lower than the one of PEEK.
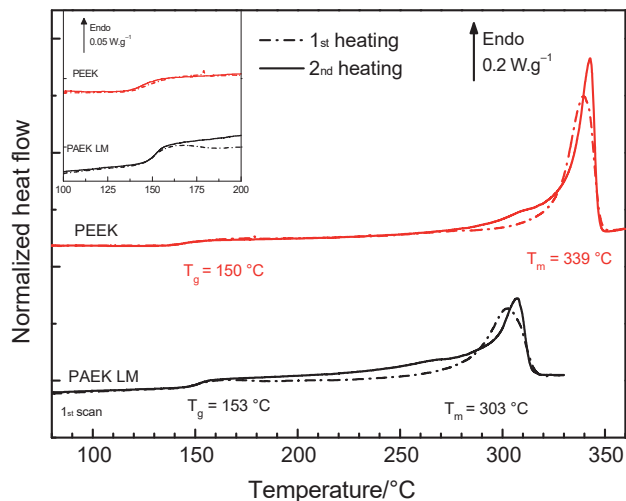
Fig. 2 DSC curves of PEEK and PAEK LM for slowly cooled samples. Dashed lines are the curves obtained after polymer processing, and solid lines are the curves obtained on the second heating scan. The inset is a blow-up on the glass transition

The value is similar to PEKK with a ratio $T/I = 60/40$, reported by Quiroga Cortes et al. [21]. The literature indicates that the variability of PEKK could be attributed to configurational defaults when terephthalic entities are replaced by isophthalic ones [27]. Only melting

temperature and thus crystallinity ratio are modified. We suggest that the PAEK LM macromolecule may contain some configurational defaults.

For each polymer, the second heating scan is identical to the first scan while the temperature is below T_g. A slight deviation should be noted on the second scan for both polymers. For PEEK, the two signals are deviating at about 270 °C ($\sim T_g + 130$ °C) instead of 165 °C ($\sim T_g + 10$ °C) for PAEK LM, indicating a relative metastability of PAEK LM. There is also a symmetry modification of the melting endotherm that is visible for both polymers. This peak is more intense indicating a remodelling of the crystallites morphology. This effect is qualitatively more important for PEEK compared with PAEK LM (Table 2).

The range between the melting temperature (heating) and the crystallization temperature (cooling) was found to be 43 and 35 °C for PAEK LM and PEEK, respectively. This result suggests an easier processing for PAEK LM.

Annealed PAEK LM

Annealing process was carried out at four different temperatures between T_g and T_m. DSC results are shown in Fig. 3. Independently from the annealing temperature, glass transition temperature of all samples increases from 151 to 154 °C. This behaviour is attributed to the reorganization of amorphous phase, although the RAF content is not different from non-annealed samples. An additional endothermic peak is also observed systematically from 10 to 20 °C above the annealing temperature. The double-melting behaviour was previously reported for PEEK [34–36] and for PEKK by Quiroga Cortes et al. [21]. No influence of the annealing temperature was observed on the value of melting peak, indicating that primary crystalline phase is not sensitive to the annealing process [16, 37]. The annealing endotherm indicates the melting of secondary crystalline phase. Their origin could be ascribed to the reorganization of amorphous phase in smaller crystallites rather than to the primary crystalline phase [37].

For PAEK LM, an increase in the annealing endotherm enthalpy is observed with the increase in annealing temperature. Lower annealing temperatures (180–200 °C) lead to low annealing enthalpy (< 2 J g^{-1}), while higher annealing temperatures (220–250 °C) generate higher endotherm enthalpy (> 3 J g^{-1}). For PEEK, Dasriaux et al. [37] suggest that the annealing temperatures below 250 °C
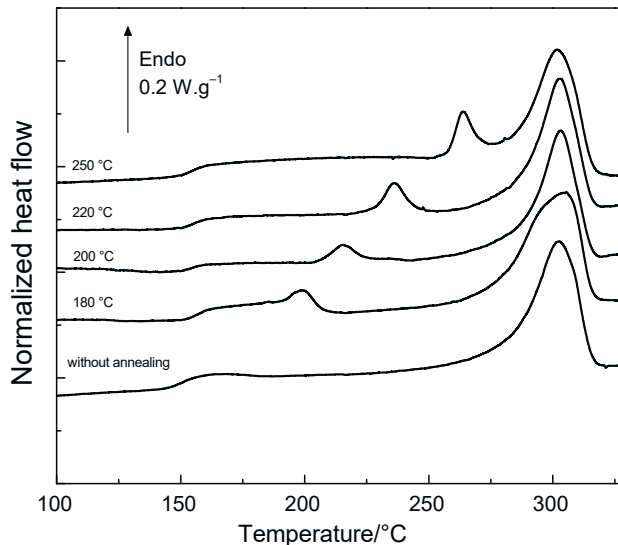

Fig. 3 DSC curves for PAEK LM after annealing at 180, 200, 220 and 250 °C

promote crystallites growth, while annealing temperatures above 250 °C promote new crystallites germination (slight increase in melting enthalpy). PAEK LM tends to have a similar behaviour to PEEK, although for annealing temperature over 250 °C, the annealing endotherm would be overlapping the melting endotherm. It is not excluded that the higher endotherm could be the result of the formation of an another crystalline morphology [36].

As a comparison, a reference annealed PEEK sample (annealing temperature of 200 °C) exhibits a lower enthalpy (~ 0.9 J g^{-1}). Consequently, there is no evolution of DSC curves upon thermal treatment. PEEK macromolecules do not undergo reorganization upon annealing as PAEK LM macromolecules do.

Thermal behaviour

Specific heat capacity

The PAEK LM- and PEEK-specific heat capacities are plotted as a function of temperature in Fig. 4. Both specific heat capacities slightly increase with temperature. Experimental data have been fitted by Eqs. (9) and (10) for PAEK LM and PEEK, respectively.

	T_g/°C	T_m/°C	ΔH_m/J g^{-1}	χ/%	T_{cryst}/°C	ΔC_p/J g^{-1}
PEEK	148 ± 2	342 ± 2	51 ± 2	38 ± 2	308 ± 2	0.12 ± 0.02
PAEK LM	151 ± 1	307 ± 1	36 ± 3	27 ± 2	265 ± 1	0.14 ± 0.05

Table 2 Transitions temperatures, melting enthalpies and crystalline ratio of slowly cooled PEEK and PAEK LM

Standard deviations were determined from the variability over various samples
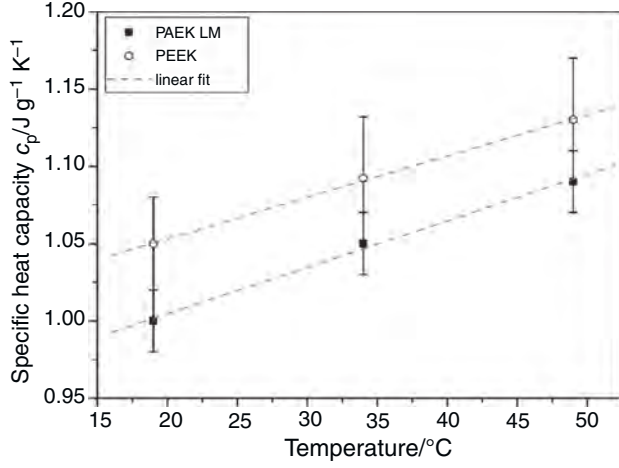
Fig. 4 Specific heat capacity measured by modulated temperature differential scanning calorimetry (MT-DSC): PAEK LM (square) and PEEK (circle). Each measure was performed on different polymeric samples. The error bars were determined from the variations over the sample, for each temperature

$$c_{p(PAEKLM)} = 0.003T + 0.94 \quad (9)$$

$$c_{p(PEEK)} = 0.003T + 1.00 \quad (10)$$

The determination of heat capacities of polymers containing phenylene groups, including PEEK, has been extensively studied by Cheng et al. [38–41]. Below the glass transition, the increase with temperature of PEEK-specific heat capacity has been associated with local mobility in the vitreous state. For macromolecules, each group vibration contributes to the total specific heat capacity. PEEK repeating unit is constituted of three phenylene groups, two ether groups (–O–) and one carbonyl group (–CO–). At 27 °C, PEEK-specific heat capacity calculated from their vibrational contribution is 1.123 J g^{-1} K^{-1} [40]. Kemmish et al. [42] reported the experimental value of 1085 J g^{-1} K^{-1} at 27 °C. These values are close to the extrapolated PEEK-specific heat capacity at 27 °C, calculated from Eq. (2) $c_{p(PEEK)}$ = 1.081 J g^{-1} K^{-1}. It appears, according to experimental results and the literature, that PAEK LM has a slightly lower specific heat capacity than PEEK. Extrapolated PAEK LM-specific heat capacity at 27 °C, calculated from Eq. (9), is $c_{p(PAEK\ LM)}$ = 1.021 J g^{-1} K^{-1}. This lower specific heat capacity could be due to configuration or spatial conformation less favourable to localized mobility compared with PEEK.

Thermal conductivity

Figure 5 displays the evolution of PAEK LM and PEEK thermal conductivities as a function of temperature. The hatched zone corresponds to the glass transition domain
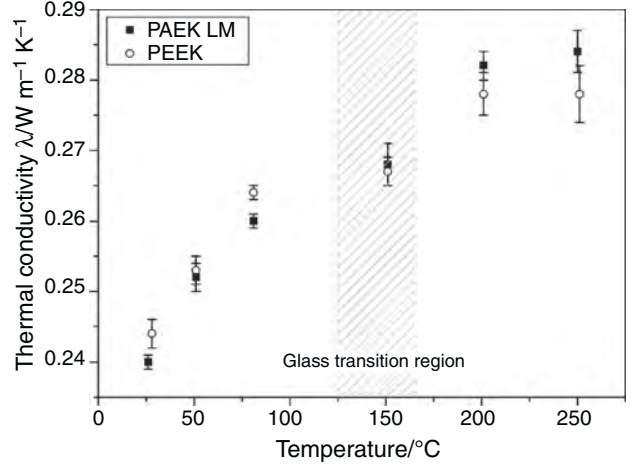

Fig. 5 Thermal conductivity measured by the guarded hot plate method: PAEK LM (square) and PEEK (circle). Errors bars are determined from the experimental standard deviation from successive measurements for each sample

($T_g \approx 145 \pm 20$ °C). For both polymers, thermal conductivity increases with temperature over the explored temperature range. Below the glass transition temperature, thermal conductivity of semi-crystalline polymers with low crystallinity ratio ($< 50\%$) increases with temperature as any disordered material [43, 44]. This behaviour is related to the heat capacity increase with temperature over the phonon mean-free path limitation with increasing temperature [45]. The thermal conductivity evolution around and above the glass transition is related to more complex mechanisms. In semi-crystalline polymers, the physical structure may evolve during measurements near or above T_g (physical ageing, crystallites reorganization). Thermal conductivity evolution is linked to the amorphous phase evolution through the balance between heat capacity increase and energy dissipation during the viscoelastic transition [46, 47]. It also depends on the crystalline phase evolution because of resistive mechanisms at crystallites/amorphous regions interfaces. In this study, thermal conductivities of PAEK LM and PEEK slightly increase with temperature above T_g indicating the dominant contribution of the heat capacity increase above T_g.

We note that thermal conductivity values of PAEK LM and PEEK are very close. Table 3 presents thermal conductivity of PAEK LM at 26 °C and PEEK at 28 °C along with values taken from the literature for PEEK. The thermal conductivity of PAEK LM falls into the same thermal conductivity range than for PEEK. These two polymers have similar thermal conductivities behaviour (magnitude and temperature evolution).

Table 3 Thermal conductivity of PAEK LM at 26 °C, PEEK at 28 °C

	Temperature/°C	Thermal conductivity/W m^{-1} K^{-1}	References
PAEK LM	26	0.240 ± 0.001	This work
PEEK	28	0.244 ± 0.002	This work
PEEK	20	0.2	Diez Pascual et al. [48]
PEEK	22	0.259	Choy et al. [49]

Comparison with the literature data for PEEK

Dynamic mechanical/dielectric relaxations

Global dynamic relaxations

Dynamic mechanical and dielectric analyses were carried out on both PEEK and PAEK LM samples after different cooling treatments. Data of slowly cooled samples are reported in Fig. 6. Conservative moduli of both polymers are shown in Fig. 6a. PAEK LM glassy and rubber moduli are lower than for PEEK. This difference has been attributed to the lower degree of crystallinity of PAEK LM as observed by DSC analysis. Contrary to PAEK LM, two consecutive PEEK curves are superimposed. For PAEK LM, an increase in the conservative modulus is observed. This evolution is more pronounced on the rubbery plateau. The crystallinity ratio of PAEK LM, controlled by DSC before each successive mechanical analysis, does not show significant variation. The increase in the modulus has been attributed to the organization of a rigid amorphous phase RAF at the periphery of crystallites [19].

The dissipative moduli are observed for both polymers, and they are reported in Fig. 6b. Two relaxation modes are pointed out. The high-temperature relaxation, labelled α, is situated at 151 and 154 °C for PEEK and PAEK LM, respectively. These values of viscoelastic relaxation are consistent with the values of T_g as measured by DSC. A low-temperature relaxation, labelled β, is observed in the range of − 100 to − 40 °C: for more clarity, it is reported in the inset of Fig. 6b. The analyses of the obtained results are separated into two sections: (1) higher temperature, in the range of the viscoelastic α relaxation; (2) lower temperature, where the sub-glass relaxation occurs.

α Relaxation

The dynamical mechanical analysis was carried out on PAEK LM samples for quenched, slowly cooled and annealed samples. Note that there are no reference PEEK data since it is not possible to make such thermal treatments to thick PEEK samples The conservative shear modulus $G'(T)$ is reported in the inset of Fig. 7. A viscoelastic relaxation α is systematically observed in the range of 140–200 °C. The thermal history has a negligible influence on the vitreous plateau ($T < 100$ °C). However, the mechanical behaviour in the region of the viscoelastic transition is strongly dependent on the thermal history. Slowly cooled samples exhibit a decrease in the conservative modulus $\Delta G'$ of 1 decade in agreement with the behaviour classically observed for semi-crystalline polymers [50]. On the contrary, the onset of viscoelastic
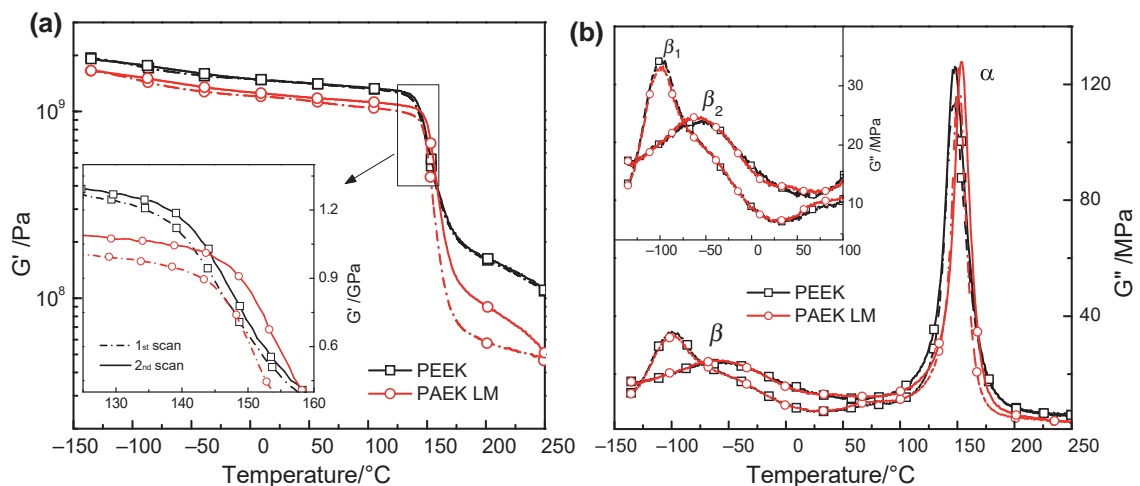

Fig. 6 Dynamic mechanical analyses of PEEK and PAEK LM. **a** Conservative modulus. Inset: Enlargement of the viscoelastic relaxation zone. **b** Dissipative modulus. Inset: Enlargement of sub-glass relaxation. First scans are represented by dashed lines; second scans are represented by the solid lines
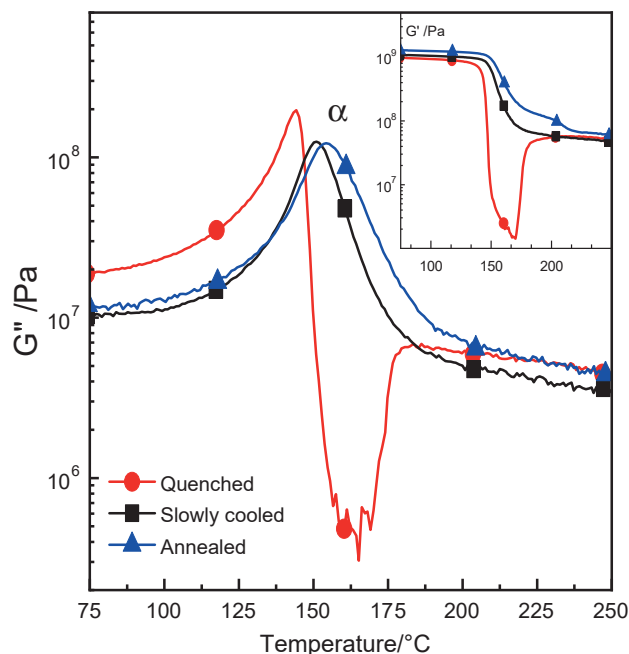
Fig. 7 Mechanical energy losses measured by dynamical mechanical analysis (DMA): quenched (circle), slowly cooled (square); and annealed (triangle) of PAEK LM. The inset shows the conservative modulus by DMA, for the same samples

Fig. 8 Arrhenius diagram of relaxation times from dynamic dielectric spectroscopy: quenched (filled circle/open circle), slowly cooled (filled square/open square) annealed (filled triangle/open triangle) for PAEK LM (filled symbols) and PEEK (open symbols). Solid lines correspond to the VTF fits. The inset reports as reference data for slowly cooled samples. Relaxation times from dynamic mechanical analysis (filled star/open star) for PAEK LM (filled symbols) and PEEK (open symbols) have been plotted for comparison

transition is observed earlier for quenched samples ($\sim$ 141 °C). The amplitude presents a decrease of 3 decades around T_α followed by a 2 decades increase starting at 170 °C. This specific mechanical behaviour—recently reported for PEKK [21]—is observed for samples with a low crystallinity. Accordingly, it has been attributed to the mechanical manifestation of a cold crystallization process above T_α. Annealed samples present a slightly higher conservative modulus on all temperature range. Excepted for quenched samples, DSC analyses were carried out on DMA samples before and after mechanical analysis. For slowly cooled and annealed samples, there is no significant variation of the crystallinity ratio. Two hypotheses are compatible with the increase in the rubbery modulus at constant crystallinity ratio: (1) thickening and/or growth of the crystalline regions and (2) increase in the rigid amorphous phase. This last one was previously reported on annealed PEEK [23, 37]. The conservative modulus of annealed samples exhibits around 215 °C, a step that might be correlated with the annealing peak observed by DSC. This correlation reinforces the hypothesis of the formation during the annealing process of secondary crystals that melt when the scanning temperature reaches the annealing temperature.

The α relaxation is located at 144, 151 and 155 °C, for quenched, slowly cooled and annealed samples, respectively (Fig. 8). For each thermal treatment, the temperature
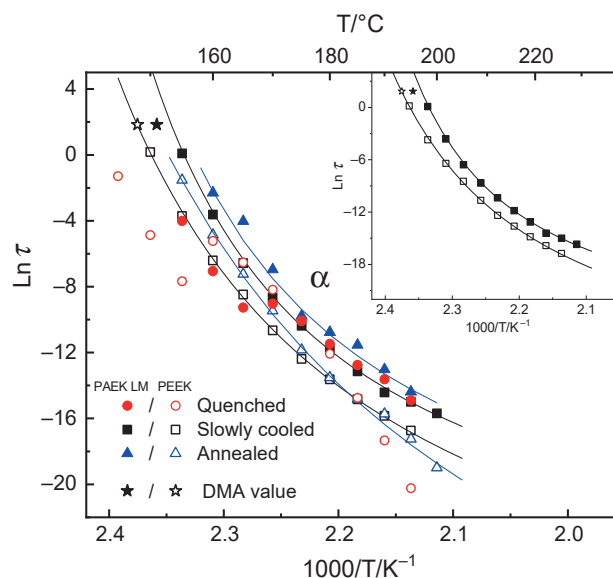
of the α mechanical relaxation is consistent with the calorimetric glass transition temperature.

Figure 8 shows an Arrhenius diagram for both PEEK and PAEK LM α relaxation, obtained by dielectric measurements for all the thermal histories. In the case of a specific thermal history, the dielectric alpha transition of PAEK LM is always observed at higher temperature than the PEEK one. These results are consistent with a higher calorimetric T_g (or T_α by DMA) analyses. Slowly cooled and annealed samples present similar α relaxation parameters that illustrate the high physical stability of the polymers. The relaxations have been fitted by a VTF equation, except for quenched samples because the crystallization process induced a perturbation on that avoided a precise determination of τ. Then, the DMA α relaxation for both polymer was added (star symbol) on the diagram (inset in Fig. 8). The corresponding relaxation times were determined as a function for the angular frequency $\tau = 2\pi/\omega$, while the temperatures were taken at the maximum of the relaxation peek (Fig. 7). An excellent correlation between both techniques for both polymer matrices is observed.

An additional dielectric relaxation is visible above the glass transition temperature from isotherms 195 to 250 °C. This mode corresponds to MWS polarization resulting from the electrical charges trapped at the interface between crystallites and amorphous phase [24]. The MWS dielectric strength is about 100 times superior to the main α

relaxation. The MWS relaxation is also described by the VTF equation for both polymers. This relaxation was previously described for PEEK [51], but no parameters were determined. Herein, we have gathered the obtained results in Table 4. The high value of $\tau_{0_{MWS}}$ is consistent with large dipoles.

β Relaxations

The low-temperature relaxation, labelled as β, shows a complex response. This relaxation was known as bimodal for PEEK [22, 52]. The evolution of mechanical relaxation upon thermal treatment can only be observed on PEEK-LM as indicated earlier. (Figure 9) The lower temperature contribution, designated as β_1, was observed by DMA (− 100 °C) and by DDS (from − 110 to 25 °C depending on frequency). We previously discussed that this relaxation was found to be visible during the first scan, while missing during the second one (inset Fig. 6b). The activation energy of 44.3 kJ mol^{-1} was determined by dielectric relaxation (Arrhenius diagram Fig. 10). Our results are consistent with the literature for PAEK [20–23, 53]. The molecular origin was previously determined to be a plasticized localized mobility of aromatic rings near polar regions due to water sorption at room temperature.

The β_2 relaxation is easily observable on dried samples, but only as a shoulder of β_1 on wet samples. Both PEEK and PAEK LM displayed the β_2 mechanical relaxation at the same temperature (− 58 °C) that strengthen the similarity of the two polymers. The literature identifies the β_2 relaxation as the localized mobility of aromatic rings in various PAEK polymers [21, 22, 54]. Quiroga et al. [21] have also observed the β_2 relaxation of PEKK which is located at higher temperature than the PEEK one, probably due to a lower proportion of Ether moieties.

The thermal treatment was found to have no influence on the mechanical position of the sub-glass relaxation of
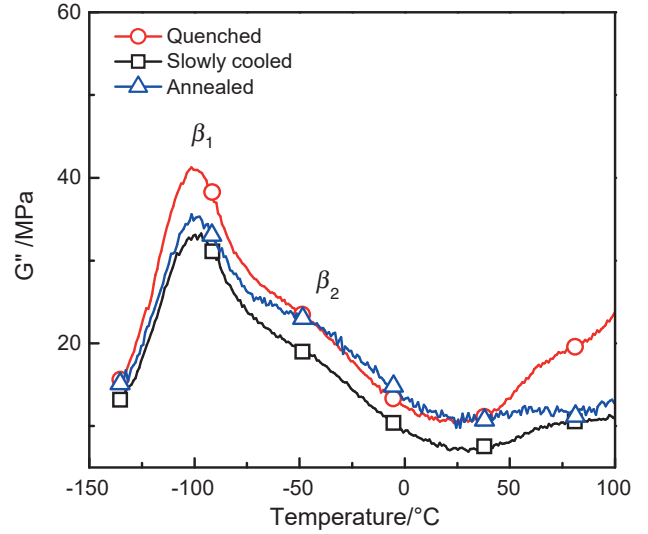

Fig. 9 Mechanical energy loss of β_1 relaxation measured by dynamic mechanical analysis for PAEK LM with different thermal histories

PAEK LM. The first mechanical scan always reveals the β_1 relaxation which is systematically observed at − 100 °C. The dielectric analyses reported in Fig. 10 show that the activation energy remains in the same range of magnitude (∼ 45 kJ mol^{-1}) for all the thermal treatments for both polymers. Our values remain consistent with the literature for PEEK [23, 54]. As there is a very similar behaviour between PEEK and PAEK LM (by DMA and DDS), the localized mobility of both polymers and their molecular origin are probably the same: oscillations of aromatic rings near polar regions interacting with water molecules. On subsequent scanning, the β_1 relaxation is not observable, indicating water desorption.

As seen in Fig. 10 and Table 4, for slowly cooled PAEKs, configurational defects have a significant influence on the parameters of the relaxation times of the β_1 relaxation. The increase of τ_0 with the percentage of defects

Table 4 Kinetic parameters of the dielectric relaxation modes for PEEK and PAEK LM

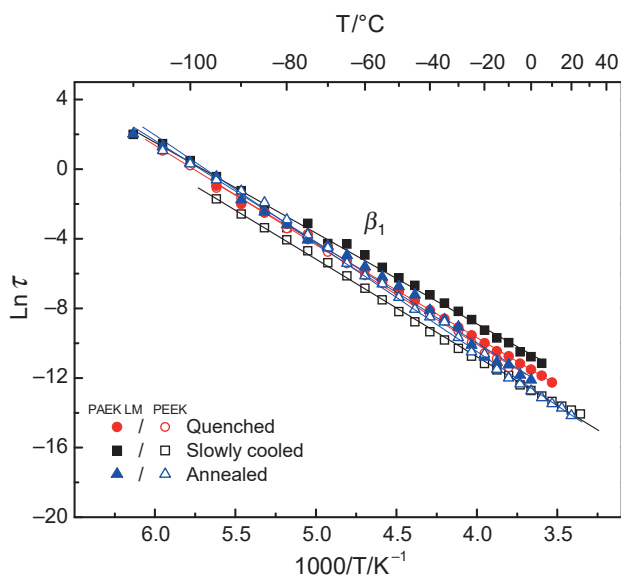| Thermal treatment	β		α			MWS		
	τ_0/s	E_a/kJ mol^{-1}	α_f/°C^{-1}	τ_0/s	T_∞/°C	α_f/°C^{-1}	τ_0/s	T_∞/°C
PAEK LM								
Quenched	2.0×10^{-15}	46.9	–	–	–	7.4×10^{-4}	2.0×10^{-6}	99
Slowly cooled	1.2×10^{-13}	44.3	8.8×10^{-4}	8.1×10^{-14}	117	7.3×10^{-4}	8.5×10^{-7}	97
Annealed	3.7×10^{-15}	51.5	1.1×10^{-3}	2.9×10^{-12}	124	1.2×10^{-3}	1.5×10^{-5}	124
PEEK								
Quenched	5.1×10^{-15}	47.5	–	–	–	6.6×10^{-4}	3.6×10^{-6}	96
Slowly cooled	3.8×10^{-15}	46.6	8.1×10^{-4}	2.0×10^{-14}	110	7.6×10^{-4}	2.1×10^{-6}	102
Annealed	4.5×10^{-16}	51.7	0.5×10^{-3}	4.7×10^{-18}	98	8.4×10^{-4}	1.9×10^{-6}	106

Fig. 10 Relaxation times of β_1 relaxation measured by dynamic dielectric spectroscopy. They are plotted on an Arrhenius diagram for PEEK (open symbols) and PAEK LM (filled symbols). Solid lines are the Arrhenius fits

from PEEK to PAEK LM indicates a localization of the molecular mobility related to configurational order for the β_1 mode.

Conclusions

Thermal, mechanical and dielectric properties of a new PAEK polymer from Victrex (AE^{TM} 250) have been analysed by calorimetry (differential and modulated) and thermal, mechanical and dielectric techniques. They have been compared to the PEEK reference. Several thermal treatments were necessary to highlight the difference between the two polymers. The PAEK LM presents a lower melting temperature (307 °C) than classical PEEK (343 °C), but the glass transition is in the same range of temperature. Moreover, the degree of crystallinity of the PAEK LM (27%) is lower than for PEEK (38%). The physical structure of the PAEK LM might involve smaller crystallites than PEEK due to a large percentage of structural defects.

The reduced melting temperature makes the processing for PAEK LM easier than for PEEK. This original behaviour was not previously reported for PEEK. The asymmetry of the PAEK LM polymer chain might be higher than for classical PEEK. The cold crystallization process was found to occur at higher temperature for PAEK LM which corroborates the hypothesis of asymmetrical defects of PAEK LM. Thermal, mechanical and dielectric behaviours of both polymers are analogous due to the similarity of the PAEK LM and the PEEK. The PAEK LM presents

the same bimodal relaxation than PEEK. Their molecular origin has been discussed. The β_1 relaxation was sensitive to the moisture content: the activation energy (45 kJ mol^{-1}) was found in the same range than for the PEEK one. The β_2 relaxation mode was found to be independent from the water content: it has been ascribed to the flip of aromatic rings between two ether moieties. The excellent correlation between the different analysis techniques allows us to improve our understanding of the physical behaviour of PEEK and PAEK LM. The thermal, mechanical and dielectric properties of PAEK LM highlight that it is possible to preserve the performance of PEEK with the advantage of a processing at lower temperature.

References

1. Panayotov IV, Orti V, Cuisinier F, Yachouh J. Polyetheretherketone (PEEK) for medical applications. J Mater Sci Mater Med. 2016;27:118.
2. Tannous F, Steiner M, Shahin R, Kern M. Retentive forces and fatigue resistance of thermoplastic resin clasps. Dent Mater. 2012;28:273–8.
3. Shaver A, Moon JD, Savacool D, Zhang W, Narang G, Miller G, et al. Poly(2,6-dimethyl-1,4-phenylene oxide) blends with a poly(arylene ether ketone) for gas separation membranes. Polym. 2017;114:135–43.
4. Díez-Pascual AM, Naffakh M, Marco C, Ellis G, Gómez-Fatou MA. High-performance nanocomposites based on polyetherketones. Prog Mater Sci. 2012;57:1106–90.
5. Yang L, Zhang S, Chen Z, Guo Y, Luan J, Geng Z, et al. Design and preparation of graphene/poly(ether ether ketone) composites with excellent electrical conductivity. J Mater Sci. 2013;49:2372–82.
6. Quiroga Cortes L, Lonjon A, Dantras E, Lacabanne C. High-performance thermoplastic composites poly(ether ketone ketone)/silver nanowires: morphological, mechanical and electrical properties. J Non Cryst Solids. 2014;391:106–11.
7. Rivière L, Lonjon A, Dantras E, Lacabanne C, Olivier P, Rocher N. Silver fillers aspect ratio influence on electrical and thermal conductivity in PEEK. Ag Nanocompos Eur Polym J. 2016;85:115–25.
8. Nohara LB, Costa ML, Alves MA, Takahashi MFK, Nohara EL, Rezende MC. Processing of high performance composites based on peek by aqueous suspension prepregging. Mater Res. 2010;13:245–52.
9. Cortes LQ, Racagel S, Lonjon A, Dantras E, Lacabanne C. Electrically conductive carbon fiber/PEKK/silver nanowires multifunctional composites. Compos Sci Technol. 2016;137:159–66.
10. Ray D, Comer AJ, Lyons J, Obande W, Jones D, Higgins RMO, et al. Fracture toughness of carbon fiber/polyether ether ketone composites manufactured by autoclave and laser-assisted automated tape placement. J Appl Polym Sci. 2014;41643:1–10.

11. Sakamoto WK, Malmonge JA, Malmonge LF, Da Silva AFG, Higuti RT. PTCa/PEEK composite acoustic emission sensors. IEEE Trans Dielectr Electr Insul. 2006;13:1177–81.

12. Vasconcelos GDC, Mazur RL, Ribeiro B, Botelho EC, Costa ML. Evaluation of decomposition kinetics of poly (ether-ether-ketone) by thermogravimetric analysis. Mater Res. 2014;17:227–35.

13. Turi E. Thermal characterization of polymeric materials. San Diego: Academic press; 1997. p. 720–1.

14. Pope JC, Sue HJ, Bremner T, Blümel J. High-temperature steam-treatment of PBI, PEEK, and PEKK polymers with H_2O and D_2O: a solid-state NMR study. Polymer. 2014;55:4577–85.

15. Zhao G, Men Y, Wu Z, Ji X, Jiang W. Effect of shear on the crystallization of the poly(ether ether ketone). J Polym Sci Part B Polym Phys. 2010;48:220–5.

16. Blundell DJ, Osborn BN. The morphology of poly(aryl-ether-ether-ketone). Polymer. 1983;24:953–8.

17. Cebe P, Hong SD. Crystallization behaviour of poly(ether-ether-ketone). Polymer. 1986;27:1183–92.

18. Krishnaswamy RK, Kalika DS. Glass transition of poly(aryl ether ketone ketone) and its copolymers. Polymer. 1996;37:1915–23.

19. Wang Y, Wang Y, Lin Q, Cao W, Liu C, Shen C. Crystallization behavior of partially melted poly(ether ether ketone). J Therm Anal Calorim. 2017;129:1021–8.

20. Krishnaswamy RK, Kalika DS. Dynamic mechanical relaxation properties of poly(ether ether ketone). Polymer. 1994;35:1157–65.

21. Quiroga Cortés L, Caussé N, Dantras E, Lonjon A, Lacabanne C. Morphology and dynamical mechanical properties of poly ether ketone ketone (PEKK) with meta phenyl links. J Appl Polym Sci. 2016;133:43396-1.

22. David L, Etienne S. Molecular mobility in para-substituted polyaryls. 1. Sub-Tg relaxation phenomena in poly(aryl-ether-ether-ketone). Macromolecules. 1992;25:4302–8.

23. Leonardi A, Dantras E, Dandurand J, Lacabanne C. Dielectric relaxations in PEEK by combined dynamic dielectric spectroscopy and thermally stimulated current. J Therm Anal Calorim. 2013;111:807–14.

24. Perrier G. Maxwell–Wagner–Sillars relaxations and crystallinity in PEEK. Compos Interfaces. 1996;4:111–7.

25. Ezquerra TA, Majszczyk J, Baltà-Calleja FJ, López-Cabarcos E, Gardner KH, Hsiao BS. Molecular dynamics of the α relaxation during crystallization of a glassy polymer: a real-time dielectric spectroscopy study. Phys Rev B. 1994;50:6023–31.

26. Smith KJ, Towle IDH, Moloney MG. Spherical, particulate poly(ether ketone ketone) by a Friedel Crafts dispersion polymerisation. RSC Adv. 2016;6:13809–19.

27. Gardner KH, Hsiao BS, Matheson RR, Wood BA. Structure, crystallization and morphology of poly (aryl ether ketone ketone). Polymer. 1992;33:2483–95.

28. In I, Kim SY. Synthesis of poly(arylene ether ketone)s containing unsymmetrical pyridyl ether linkages. Polym Bull. 2006;56:129–35.

29. Wunderlich B, Jin Y, Boller A. Mathematical description of differential scanning calorimetry based on periodic temperature modulation. Thermochim Acta. 1994;238:277–93.

30. Thomas LC. Measurement of accurate heat capacity values. TA Instruments, Modul. DSC Pap. #9. 2005; p. 1–11.

31. Havriliak S, Negami S. A complex plane analysis of α-dispersions in some polymer systems. J Polym Sci Part C Polym Symp. 2007;14:99–117.

32. Cser F, Goodwin A. Structural studies on PEK/TPI blends. J Therm Anal Calorim. 2001;65:69–86.

33. Xu H, Ince BS, Cebe P. Development of the crystallinity and rigid amorphous fraction in cold-crystallized isotactic polystyrene. J Polym Sci Part B Polym Phys. 2003;41:3026–36.

34. Lee Y, Porter RS. Double-melting behavior of poly(ether ether ketone). Macromolecules. 1987;20:1336–41.

35. Wei CL, Chen M, Yu FE. Temperature modulated DSC and DSC studies on the origin of double melting peaks in poly(ether ether ketone). Polymer. 2003;44:8185–93.

36. Marand H, Prasad A. On the observation of a new morphology in poly(arylene ether ether ketone). A further examination of the double endothermic behavior of poly(arylene ether ether ketone). Macromolecules. 1992;25:1731–6.

37. Dasriaux M, Castagnet S, Thilly L, Chocinski-Arnault L, Boyer SAE. Evolution of the amorphous fraction of PEEK during annealing at atmospheric and high pressure above the glass transition temperature. J Appl Polym Sci. 2013;130:1148–57.

38. Cheng SZD, Cao M, Wunderlich B. Glass transition and melting behavior of Poly(oxy-1,4-phenyleneoxy-1,4-phenylenecarbonyl-1,4-phenylene). Macromolecules. 1986;19:1868–76.

39. Cheng SZD, Wunderlich B. Heat capacities and entropies of liquid, high-melting-point polymers containing phenylene groups (PEEK, PC and PET). J Polym Sci Part B Polym Phys. 1986;24:1755–65.

40. Cheng SZD, Lim S, Judovits LH, Wunderlich B. Heat capacities of high melting polymers containing phenylene groups. Polymer. 1987;28:10–22.

41. Cheng SZD, Wunderlich B. Thermal analysis of thermoplastic polymers. Thermochim Acta. 1988;134:161–6.

42. Kemmish DJ, Hay JN. The effect of physical ageing on the properties of amorphous PEEK. Polymer. 1985;26:905–12.

43. Choy CL. Thermal conductivity of polymers. Polymer. 1977;18:984–1004.

44. Choy CL, Ong EL, Chen FC. Thermal diffusivity and conductivity of crystalline polymers. J Appl Polym Sci. 1981;26:2325–35.

45. Zeller RC, Pohl RO. Thermal conductivity and specific heat of noncrystalline solids. Phys Rev B. 1971;4:2029–41.

46. Dashora P, Gupta G. On the temperature dependence of the thermal conductivity of linear amorphous polymers. Polymer. 1996;37:231–4.

47. Bafna M, Dashora P. A theoretical study of temperature dependence of thermal diffusivity of linear amorphous and semicrystalline polymers. Int J Recent Sci Res. 2012;3:417–22.

48. Díez-Pascual AM, Guan J, Simard B, Gómez-Fatou MA. Poly(phenylene sulphide) and poly(ether ether ketone) composites reinforced with single-walled carbon nanotube buckypaper: II—Mechanical properties, electrical and thermal conductivity. Compos Part A Appl Sci Manuf. 2012;43:1007–15.

49. Choy CL, Kwok KW, Leung WP, Lau FP. Thermal conductivity of poly(ether ether ketone) and its short-fiber composites. J Polym Sci Part B Polym Phys. 1994;32:1389–97.

50. Capsal J-F, Pousserot C, Dantras E, Dandurand J, Lacabanne C. Dynamic mechanical behaviour of polyamide 11/barium titanate ferroelectric composites. Polymer. 2010;51:5207–11.

51. Arous M, Ben AI, Kallel A, Fakhfakh Z, Perrier G. Crystallinity and dielectric relaxations in semi-crystalline poly(ether ether ketone). J Phys Chem Solids. 2007;68:1405–14.

52. Sasuga T, Hagiwara M. Molecular motions of non-crystalline poly(aryl ether-ether-ketone) PEEK and influence of elecron beam irradiation. Polymer. 1985;26:501–5.

53. Goodwin A, Hay J. Dielectric and dynamic mechanical relaxation studies on poly (aryl ether ketone) s. J Polym Sci Part B Polym Phys. 1998;36:851–9.

54. Goodwin A, Marsh R. Dielectric and dynamic mechanical relaxation of poly(ether ether ketone)/poly(etherimide) blends below the glass transition. Macromol Rapid Commun. 1996;17:475–80.